Published in Swiss Journal of Geosciences, 106, issue 1, 63-78, 2013
which should be used for any reference to this work

Thermal structure and metamorphic evolution of the Piemont-Ligurian metasediments in the northern Western Alps

François Negro · Romain Bousquet · Flurin Vils · Clara-Marine Pellet · Jeanette Hänggi-Schaub

Abstract In the Western Alps, the Piemont-Ligurian oceanic domain records blueschist to eclogite metamorphic conditions during the Alpine orogeny. This domain is classically divided into two "zones" (Combin and Zermatt-Saas), with contrasting metamorphic evolution, and separated tectonically by the Combin fault. This study presents new metamorphic and temperature (RSCM thermometry) data obtained in Piemont-Ligurian metasediments and proposes a reevaluation of the P–T evolution of this domain. In the upper unit (or "Combin zone") temperatures are in the range of 420–530 °C, with an increase of temperature from upper to lower structural levels. Petrological evidences show that these temperatures are related to the retrograde path and to deformation at greenschist metamorphic conditions. This highlights heating during exhumation of HP metamorphic rocks. In the lower unit (or "Zermatt-Saas zone"), temperatures are very homogeneous in the range of 500–540 °C. This shows almost continuous downward temperature increase in the Piemont-Ligurian domain. The observed thermal structure is interpreted as the result of the upper and lower unit juxtaposition along shear zones at a temperature of ~500 °C during the Middle Eocene. This juxtaposition probably occurred at shallow crustal levels (~15–20 km) within a subduction channel. We finally propose that the Piemont-Ligurian Domain should not be viewed as two distinct "zones", but rather as a stack of several tectonic slices.

Keywords RSCM thermometry · Zermatt-Saas · Combin · Cignana · HP and UHP metamorphism

F. Negro (✉) · C.-M. Pellet
Centre d'Hydrogéologie et de Géothermie,
Université de Neuchâtel, Emile Argand 11,
2000 Neuchâtel, Switzerland
e-mail: francois.negro@unine.ch

R. Bousquet · J. Hänggi-Schaub
Institut für Geowissenschaften, Universität Potsdam,
Karl-Liebknecht Strasse. 24, 14476 Potsdam-Golm, Germany

F. Vils
School of Earth Sciences, University of Bristol, Wills Memorial Building, Queen's Road, Bristol BS8 1RJ, UK

1 Introduction

The northern part of the Western Alps, located between the Rhoˆne-Simplon and the Aosta-Ranzola faults, represent a ''transition'' zone where many paleogeographic domains were continuously accreted within the alpine orogenic wedge. Within this orogenic wedge, the Piemont-Ligurian oceanic domain recorded blueschist to eclogite facies metamorphic conditions during the Alpine orogeny. The Piemont-Ligurian zone is classically divided, according to their metamorphic evolution, into a greenschist to blueschist facies unit (Combin zone), and an eclogite to UHP facies unit (Zermatt-Saas zone) (e.g. Bearth 1976; Dal Piaz 1988; Balle`vre and Merle 1993). Much attention has been paid to the metamorphic evolution of the HP to UHP Zermatt-Saas zone because of well-preserved eclogite facies assemblages in metabasites (e.g. Bearth 1967; Ernst and Dal Piaz 1978; Oberha¨nsli 1980; Barnicoat and Fry 1986; Bucher et al. 2005), coesite inclusions within garnets in metaradiolarites (Reinecke 1991) and micro-diamonds in metamorphosed seafloor Mn nodules (Frezzotti et al. 2011). The Combin zone contains only few relics of blueschist facies assemblages in both metabasites (Ayrton

et al. 1982; Sperlich 1988; Bucher et al. 2004) and metapelites (Pfeifer et al. 1991; Bousquet et al. 2004), which makes its metamorphic evolution difficult to assess. The contact between both zones is interpreted as a major contact, known as the Combin fault (Balle`vre and Merle 1993), that played an important role in the exhumation of HP metamorphic rocks within the orogenic wedge (e.g. Reddy et al. 1999; Froitzheim et al. 2006). However, the limit between both zones is sometimes difficult to define in the field (e.g. Cartwright and Barnicoat 2002; Bucher et al. 2004).

In order to better constrain the metamorphic evolution of the Piemont-Ligurian domain, we investigated the temperature record in the oceanic metasediments of the different units, using Raman spectroscopy of carbonaceous material (RSCM, Beyssac et al. 2002). This method allows quantifying the maximum temperature reached during the metamorphic evolution. As carbonaceous material is ubiquitous in metasediments in the area of investigation, this method is particularly suitable for quantifying the metamorphic evolution. We also analysed the metamorphic assemblages in metasediments, in order to correlate the estimated temperatures with P–T evolution of the different units. Samples were collected in the northern Western Alps at different structural levels of the Combin zone, across the Combin fault, and in the Zermatt-Saas zone.

We present in this work a combined petrological and RSCM study. Results of 62 RSCM temperatures obtained in the Combin and Zermatt-Saas zones in the northern part of the Western Alps are compared with new data on the metamorphic evolution of the Piemont-Ligurian units. The distribution of temperatures is discussed in the frame of the nappe structure and the P–T evolution of the Piemont-Ligurian units in the northern Western Alps.

2 Geological setting

2.1 Regional geology

The study area is located in the northern part of the Western Alps. This region is characterised by a nappe-stack of different protolithic and paleogeographic origin (Fig. 1):

- oceanic derived units: the Sion-Courmayeur zone from the Valaisan ocean, and the Tsaté and Zermatt-Saas units from the Piemont-Ligurian ocean.
- continent derived units: the Grand St. Bernard nappe system and the Monte Rosa nappe from the Briançonnais microcontinent, and the Dent Blanche nappe and the Sesia zone from the Apulian margin.

The Piemont-Ligurian domain, is a structurally composite domain which is classically divided in two "zones" based on stratigraphic, tectonic and metamorphic criteria: an upper unit, also called ''Combin zone'', and a lower unit, the ''Zermatt-Saas zone'' (e.g. Dal Piaz 1965; Bearth 1967, 1976; Dal Piaz and Ernst 1978; Sartori 1987; Dal Piaz 1988). In the following we will describe the main characteristics of both units, mainly on the stratigraphic, tectonic and metamorphic descriptions available in the Western Swiss Alps, underlining the correlation of units with the Italian Alps (Aosta valley).

2.2 The upper unit or "Combin zone"

Since the work of Argand (1909), who introduced the term of ''Combin zone'', several studies related to the stratigraphy and the internal structure of this zone have been published (e.g. Bearth 1976; Marthaler 1984; Sartori 1987; Dal Piaz 1988; Escher et al. 1993; Sartori and Marthaler 1994). However, there are still different interpretations regarding the internal structure and the tectonic evolution of this complex zone. The upper unit (UU) is composed of several tectonic nappes of different paleogeographic origin.

The Tsate´ nappe (Sartori 1987) mainly consists of oceanic rocks: metagabbros, serpentinites, metabasites, calcschists and marbles of Jurassic-Cretaceous age. The metabasites and metasediments of the Tsate´ nappe show few occurrences of mineral assemblages indicating HP metamorphism. Sodic amphibole (glaucophane or crossite) and lawsonite relics, sometimes associated with garnet, have been described locally in metagabbros, metabasalts and prasinites (Dal Piaz and Ernst 1978; Ayrton et al. 1982; Sperlich 1988; Vannay and Alleman 1990; Cartwright and Barnicoat 2002; Bucher et al. 2004). Carpholite pseudomorphs have also been described in the calcschists located NW of the Dent Blanche nappe (Pfeiffer et al. 1991), as well as relics of garnet, Mg-rich chloritoid and phengite in the Zermatt area (Bousquet et al. 2004, 2008). Maximum P–T conditions are however still poorly documented. The available estimates are in the range of 9–12 kbar and 300–475 °C for metabasites (Reddy et al. 1999; Cartwright and Barnicoat 2002) up to 15 kbar and 450 °C in metasediments (Bousquet et al. 2008).

At the base of the Tsate´ nappe, or sometimes intermingled inside the Tsate´ nappe, occur discontinuous exotic sheets: the Cimes Blanches (Pancherot-Cime Bianche unit in the northern Aosta valley) and Frilihorn nappes (Dal Piaz 1988; Escher et al. 1993). They mainly consist of rocks of continental origin: quartzites, schists, marbles, dolomites and conglomerates of Permian to Cretaceous age. These nappes are interpreted as exotic decollement sheets derived from Mesozoic continental cover sequences of the Brianc¸onnais domain (Marthaler 1984; Sartori 1987; Dal Piaz 1988; Vannay and Alleman 1990; Escher et al. 1993) that were incorporated during early stages of

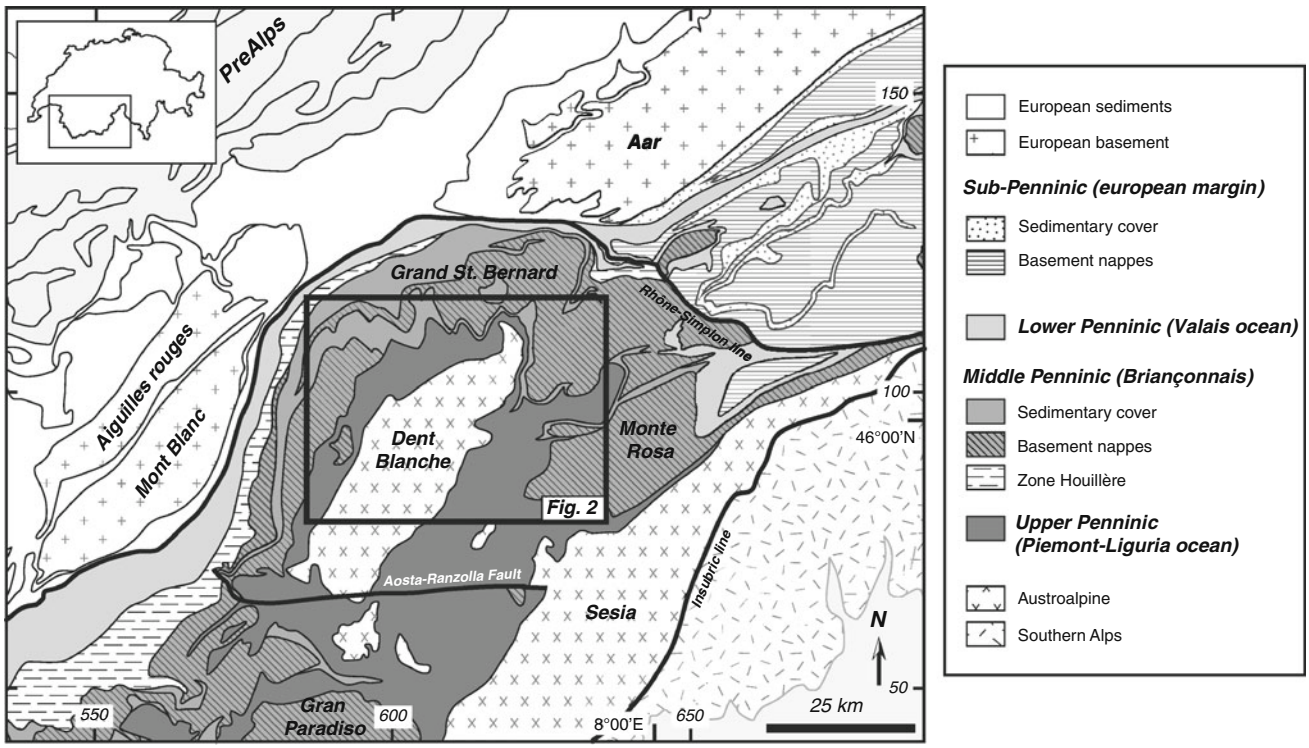

Fig. 1 Tectonic map of the northern Western Alps, modified after Bousquet et al. (2012b)

formation of the Piemont-Ligurian accretionary prism (Marthaler and Stampfli 1989; Sartori and Marthaler 1994). Other studies also propose that the Frilihorn and Cimes Blanches nappes are derived from the Mesozoic sedimentary cover of the Sesia-Dent Blanche basement nappes, incorporated within the accretionary prism during early stages of deformation (Froitzheim et al. 2006; Pleuger et al. 2007). According to Escher et al. (1993) and Steck et al. (1999), the Cimes Blanches nappe is considered to represent the base of the UU, which overlies the Grand St. Bernard nappe system to the north and the Zermatt-Saas zone to the south. These rocks locally display jadeite-quartz-phengite mineral assemblages (Bousquet et al. 2004).

2.3 The lower unit or "Zermatt-Saas zone"

The lower unit (LU), or Zermatt-Saas zone (ZSZ), consists of an ophiolite sequence derived from the Piemont-Liguria Ocean and composed of metaperidotites, metagabbros, metabasalts and serpentinites (Bearth 1967) of middle Jurassic age (Rubatto et al. 1998). An oceanic sedimentary cover mainly composed of metapelites, marbles and metacherts of Jurassic-Cretaceous age (Bearth 1967, 1976; Bearth and Schwander 1981; Dal Piaz 1965) completes the sequence. This zone is considered either as a homogeneous unit (Angiboust et al. 2009) or, based on the different metamorphic evolutions, as an assemblage of several tectonic slices (Bousquet et al. 2008; Groppo et al. 2009).

The typical HP-metamorphic assemblages in metabasalts and metagabbros of the ZSZ are composed of garnet-omphacite-glaucophane ± chloritoid ± talc, first described in the Zermatt area (Bearth 1959), documenting maximum P–T conditions in the range of 16–20 kbar and 550–600 °C (e.g. Ernst and Dal Piaz 1978; Oberha¨nsli 1980; Barnicoat and Fry 1986). Despite no new petrological findings, these P–T conditions were recently revaluated to upper values ~23–27 kbar and ~550–600 °C on the basis of new thermobarometric calculations (Bucher et al. 2005; Angiboust et al. 2009). Furthermore, the discovery of coesite inclusions within garnet in metasediments at Lago di Cignana, indicate locally UHP conditions of 27–32 kbar and 590–630 °C (Reinecke 1991, 1998; Groppo et al. 2009). More recently, microdiamonds were discovered in some garnets of the Lago di Cignana UHP unit, indicating pressures over 32 kbar (Frezzotti et al. 2011). The UHP Cignana unit, composed of large boudins of metabasalts and metagabbros embedded in metasediments, is located in the upper part of the LU (Forster et al. 2004; Groppo et al. 2009).

2.4 Structure of the Piemont-Ligurian nappe stack

The difference in metamorphic record between the UU and the LU led some authors to propose the existence of a

major tectonic contact in between, known as the Combin fault (Balle`vre and Merle 1993) or Gressoney Shear Zone in the Aosta valley (Reddy et al. 1999). The nature of this contact (i.e. extensional and/or compressional), the amount of displacement and its role in the exhumation of HP Piemont-Ligurian units is still widely debated (Reddy et al. 1999, 2003; Froitzheim et al. 2006; Pleuger et al. 2007). Studies realised in the vicinity of this contact underline that a distinction of both units is difficult to assess due to per-vasive retrogression and deformation (Cartwright and Barnicoat 2002; Groppo et al. 2009). Most of the authors locate the limit between the UU and the LU (i.e. the Combin fault) at the base of the Cimes Blanches nappes (Escher et al. 1993; Balle`vre and Merle 1993; Reddy et al. 2003; Pleuger et al. 2007). However other studies locate the contact lower than the base the Cimes blanches nappe (or Pancherot-Cime Bianche unit) in the Zermatt region and the northern Aosta valley (Compagnoni and Rolfo 2003; Bucher et al. 2004; Forster et al. 2004). In addition to lithological differences, the distinction between the UU and the LU is frequently based on the estimated metamorphic record in metabasites. Most of the studies distinct the two units by the presence or absence of eclogite facies mineral assemblages (Balle`vre and Merle 1993; Ring 1995; Reddy et al. 1999, 2003; Pleuger et al. 2007; Beltrando et al. 2008). The UU is considered to be greenschist (Balle`vre and Merle 1993; Reddy et al. 1999) to blueschist facies (Bousquet 2008; Bousquet et al. 2012a).

3 Methodology

During diagenesis and metamorphism, carbonaceous material (CM) present in the initial sedimentary rock is progressively transformed into graphite (graphitization). Because of the irreversible character of graphitization, CM structure primarily depends on the maximum temperature reached during the metamorphic cycle, and is therefore not sensible to retrograde or subsequent evolution at lower temperature (Wopenka and Pasteris 1993; Beyssac et al. 2002). A linear correlation between the structural organisation of CM, measured by Raman spectroscopy, and the metamorphic temperature has been calibrated (RSCM method—Beyssac et al. 2002). The calibration was made using samples from different regional metamorphic belts with well-known P–T conditions, and allows the determination of temperatures in the range of 330–650 °C with a calibration accuracy estimated to ±50 ° C. The relative uncertainties on temperature are much smaller, allowing high resolution field mapping of temperatures (Negro et al. 2006; Wiederkehr et al. 2011). Other calibrations have also been published to extend this temperature range below 330 ° C (Rahl et al. 2005; Lahfid et al. 2010) or for rocks affected by regional metamorphism (Aoya et al. 2010). These other calibrations were done on different Raman spectrometers with different laser wavelength. This may significantly affect the estimated temperatures (Aoya et al. 2010). We only used the original calibration and analytical setup of Beyssac et al. (2002) in this study.

Raman spectra were performed on a Renishaw InVIA reflex microspectrometer (Laboratoire de Ge´ologie, ENS Paris, and IMPMC Paris, France) equipped with a 514 nm Spectra Physics (20 mW) argon laser. Laser beam was focused on the sample using a DMLM Leica microscope with a 100 × objective (NA = 0.90), with laser power at sample surface of ∼1 mW. The signal was filtered by edge filters and dispersed with a 1,800g/mm grating to be ana-lysed by a Peltier cooled RENCAM CCD detector. Before each session the spectrometer was calibrated with a silicon standard. Because Raman spectroscopy of CM can be affected by several analytical mismatches, we followed closely the analytical and fitting procedures described by Beyssac et al. (2002, 2003). Measurements were only performed below transparent minerals, generally quartz, to avoid any effect of polishing on the structure of CM (Beyssac et al. 2003). For each sample, 10–24 spectra were recorded in order to smooth out the within-sample struc-tural heterogeneity. Spectra were processed using the Peakfit software following the procedure described in Beyssac et al. (2003).

4 RSCM temperatures in the Piemont-Ligurian units

The 62 samples were collected in the Piemont-Ligurian domain in 3 different areas (Fig. 2): North of the Dent Blanche nappe, in the Zermatt area and in the Lago di Cignana area. Among these samples, 50 were collected in the UU, and 12 in the LU, in order to highlight thermal structure of the Piemont-Ligurian nappe stack. For each sample, we also described the observed mineral assemblage in order to give a comparison with our estimated temperature (Figs. 2, 3, 6; Table 1).

4.1 Zermatt area

Samples were collected along different profiles in the Zermatt area across the two units (Fig. 3). A subset of representative spectra is depicted in Fig. 4.

4.1.1 Upper unit

The Raman spectra in the metasediments of the UU show significant variation in the CM structural organisation

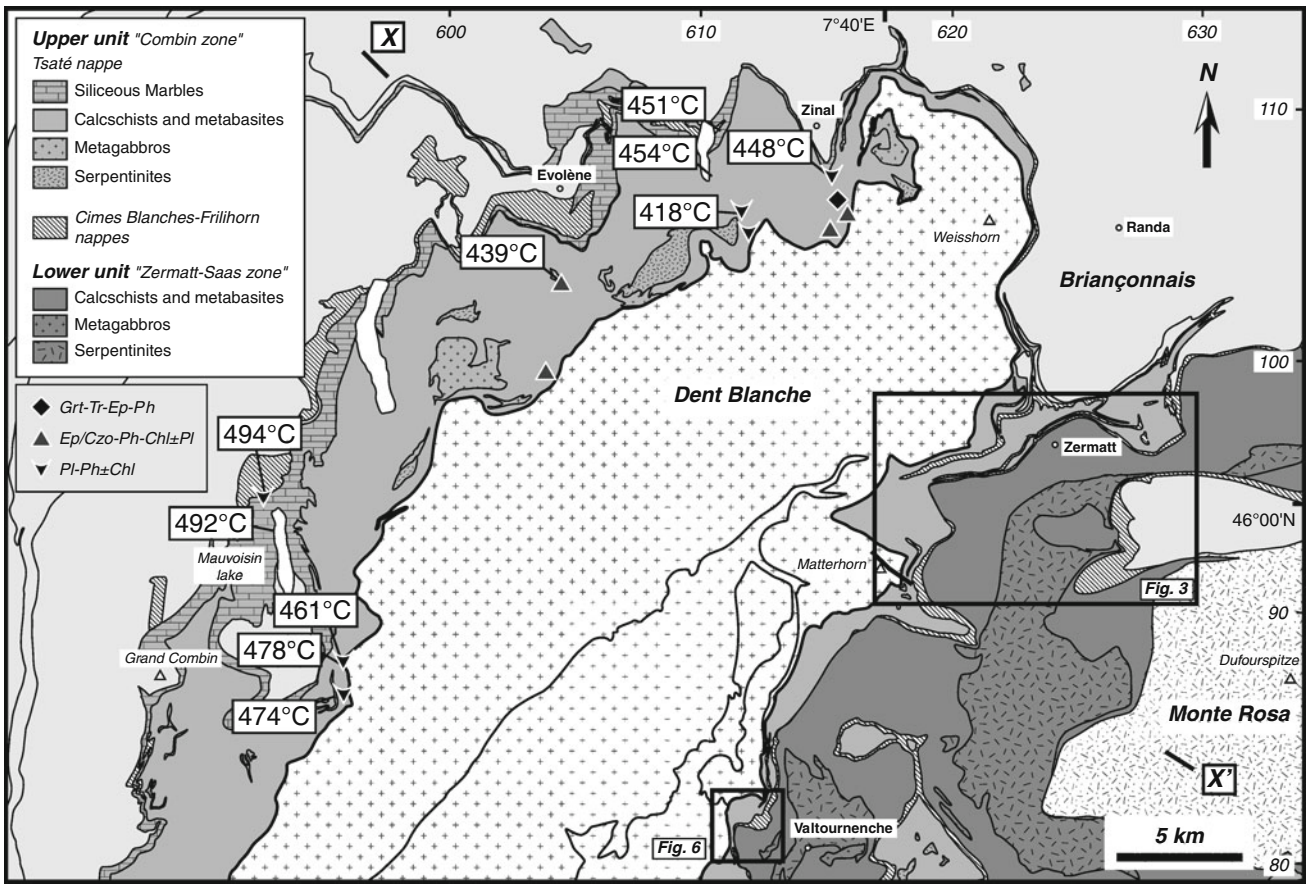

Fig. 2 Tectonic map of the Piemont-Ligurian units around the Dent Blanche massif (modified after Steck et al. 1999) showing RSCM temperatures and mineral assemblages in the upper unit of the Piemont-Ligurian domain. The absolute uncertainty on RSCM temperatures is ±50 °C. The map is located in Fig. 1

(Fig. 4). The degree of organization increases from upper to lowermost levels, with a variation of the R2 ratio from 0.50 to 0.25 (Table 1).

Along the profile below the Matterhorn, from Ho¨rnli-hu¨tte to Schwarzsee, temperature increases from ∼450 °C at the contact with the Matterhorn Austro-Alpine units to 500–530 °C near the contact with the LU (Figs. 3, 5a). However, temperatures are mainly in the range 450–475 °C along this profile. The profile located from Trift to Zermatt shows very homogeneous temperature record in the range of 480–500 °C, except for one sample that shows a temperature of 420 °C (Figs. 3, 5b). Samples collected in the Oberrothorn area also show homogeneous temperature record ranging from 500 to 520 °C, similar to the Ho¨rnlihu¨tte-Schwarzsee and Trift-Zermatt profiles (Fig. 3).

4.1.2 Lower unit

The spectra obtained in the LU are very homogeneous, with an R2 ratio in the range 0.22–0.33 indicating that the CM is generally well-ordered in this unit (Fig. 4; Table 1). Estimated temperatures are always in the range of ∼500–540 °C across the whole area, showing homogeneous peak T record in the metasediments of this unit (Fig. 3).

4.2 Lago di Cignana

Samples were collected along a NW–SE transect across the UU, and across the contact between the two units (Fig. 6). The Raman spectra are very similar to the Zermatt area, with relatively well ordered CM and R2 ratios in the range 0.25–0.42 (Table 1).

Along the NNW-SSE profile passing through Mt. Pancherot, temperature increases from ∼460–470 °C in uppermost sampled levels of the UU, to ∼530 °C at the contact with the underlying LU (Fig. 6b). A single sample collected north of the Lago di Cignana shows temperature of ∼475 °C similar to the ones observed along the profile (Fig. 6a). Samples collected near the contact, W of Lago di Cignana, show similar temperatures of ∼510–520 °C in both the UU and the LU. Finally, one sample collected in the LU shows temper-ature of ∼540 °C, very similar to the temperatures observed near the contact further north (Fig. 6a).

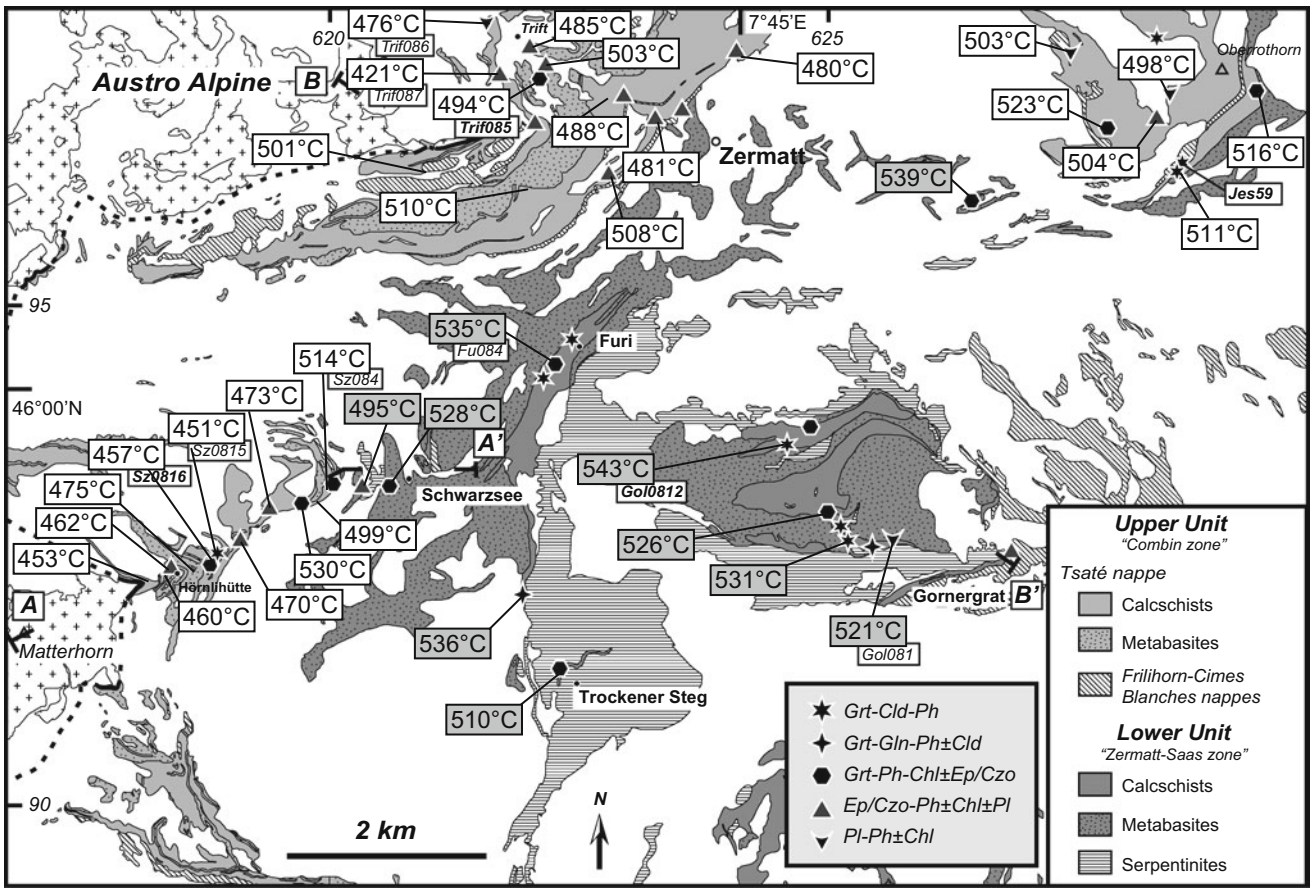

Fig. 3 Tectonic map of the Zermatt area (modified after Bearth 1953 and Bucher et al. 2003) with RSCM temperatures and mineral assemblages in the upper and lower units of the Piemont-Ligurian domain. The absolute uncertainty on RSCM temperatures is ±50 °C. The map is located in Fig. 2

4.3 North of the Dent Blanche nappe

Samples were collected in the metasediments of the UU in different N–S valleys and around barriers lakes (Fig. 2). The Raman spectra are very similar to those observed within the UU in the Zermatt and Lago di Cignana areas, with relatively well ordered CM and R2 ratios in the range 0.33–0.50 (Table 1). Temperatures are slightly lower in the Evole`ne-Zinal area, in the range 420–450 ° C, compared to the Mauvoisin lake area where they are in the range 460–500 ° C. However these temperatures are in good agreement with those observed SE of the Dent Blanche massif, showing spatially coherent distribution of temper-atures in the whole UU.

4.4 RSCM temperatures and Piemont-Ligurian nappe structure

We have reported the range of estimated RSCM temperatures on a simplified geological cross section of the studied area (Fig. 7) in order to assess the relation between the estimated temperatures and the Piemont-Ligurian nappe structure. These temperature ranges correspond to a synthesis of observations in the three studied areas, and have been projected on the cross section according to the structural position of the samples in the UU.

The RSCM temperatures in the UU show coherent distribution (Fig. 7). In the upper structural levels of the UU temperatures are in the range of 420–470 ° C, observed below the contact with the Dent Blanche nappe. Interme-diate levels, which have been intensely folded, as underlined by the position and the structure of the Frilihorn nappe, show temperatures in the range of 470–500 ° C. In the lower structural levels of the UU, close to the contact with the LU, temperatures are in the range of 500–530 ° C. These latter temperatures are quite similar to those observed in the underlying LU, in the range of 500–540 ° C. The temperatures observed north of the Dent Blanche nappe, in contact with the underlying Grand St. Bernard nappe system, are slightly lower, in the range of 470–500 °C.

Table 1 Samples from the Piemont-Ligurian units with coordinates (CH1903) and elevation, observed mineral assemblages, number of Raman spectra (Sp.), R2 ratio (mean value and standard deviation) and RSCM temperature (mean value and 1-σ uncertainty)

Coord. (CH1903)						R2 ratio		Temperature (°C)		
Zone/Unit	Sample	X	Y	Elev. (m)	Mineral assemblage	Sp	Mean	SD	Mean	1 s
N Dent Blanche										
Upper unit	CO0701	615,058	107,391	1,710	Ph-Chl-Pl-Cal-Qz	10	0.43	0.02	448	3
	CO0702	615,330	106,064	1,741	Grt-Tr-Phg	–	–	–	–	–
	CO0703	611,196	105,737	2,298	Ep-Ph-Cal-Qtz	–	–	–	–	–
	CO0705	61,0368	10,7249	2,308	Ph-Cal-Qz	12	0.42	0.04	454	5
	CO0706	61,0668	10,9121	2,266	Ph-Chl-Cal-Qz	12	0.43	0.03	451	5
	CO0708	595,613	88,050	2,599	Ph-Chl-Pl-Cal-Qz	11	0.41	0.03	461	4
	CO0709	595,611	88,037	2,581	Ph-Chl-Pl-Cal-Qz	12	0.37	0.04	478	5
	CO0710	595,453	86,667	2,321	Ph-Chl-Pl-Cal-Qz	19	0.37	0.07	477	7
	CO0711	592,929	93,290	2,059	Ph-Chl-Cal-Qz	12	0.33	0.06	492	8
	CO0712	592,460	94,576	1,849	Ph-Chl-Pl-Cal-Qz	24	0.33	0.07	494	7
	CO0901	603,724	99,591	1,823	Ep-Ph-Chl-Pl-Qz	–	–	–	–	–
	CO0902	604,401	103,221	1,769	Czo/Ep-Pl-Ph-Chl-Cal-Qz	12	0.45	0.03	439	4
	CO0904	615,111	105,507	1,890	Ep-Ph-Chl-Pl-Qz	–	–	–	–	–
	CO0906	611,996	105,029	2,596	Ph-Chl-Pl-Cal-Qz	–	–	–	–	–
	CO0907	61,1436	105,801	2,499	Ph-Chl-Pl-Cal-Qz	10	0.50	0.03	418	4
Zermatt										
Upper unit	SZ084	619,963	93,124	2,787	Ph-Chl-Cal-Qz	11	0.29	0.05	514	7
	SZ085	618,593	92,337	3,171	Ph-Chl-Cal-Qz	15	0.37	0.04	475	4
	SZ087	618,409	92,325	3,257	Czo/Ep-Ph-Chl-Pl-Qz	12	0.40	0.02	462	3
	SZ088	618,351	92,305	3,262	Ph-Cal-Qz	15	0.41	0.04	460	5
	SZ089	618,259	92,231	3,254	Ph-Cal-Qz	11	0.42	0.06	453	7
	SZ0810	619,888	93,013	2,870	Ph-Cal-Qz	10	0.32	0.06	499	8
	SZ0811	619,390	92,963	2,940	Ep-Chl-Ph-Pl-Cal-Qz	12	0.38	0.03	473	4
	SZ0812	619,720	92,981	2,865	Grt-Ep-Chl-Ph-Qz	10	0.25	0.07	530	9
	SZ0814	618,904	92,560	3,000	Ep-Chl-Ph-Pl-Cal-Qz	12	0.38	0.03	470	4
	SZ0815	618,874	92,492	3,100	Grt-Cld-Ep-Ph-Pl-Cal-Qz	12	0.43	0.03	451	4
	SZ0816	618,852	92,502	3,200	Grt-Ep-Ph-Pl-Qz	15	0.42	0.04	457	5
	HB081	623,465	96,914	1,800	Ph-Pl-Cal-Qtz	–	–	–	–	–
	HB083	622,817	96,313	2,095	Czo/Ep-Ph-Chl-Cal-Qz	10	0.30	0.04	508	5
	HB088	621,969	96,148	2,480	Ph-Cal-Qz	10	0.30	0.04	510	5
	HB0811	621,000	96,335	2,786	Ph-Cal-Qz	12	0.31	0.07	501	8
	TRIF081	623,224	96,832	1,895	Ep-Ph-Chl-Pl-Cal-Qtz	11	0.36	0.03	481	4
	TRIF082	622,921	97,067	1,974	Ep-Ph-Chl-Pl-Cal-Qtz	–	–	–	–	–
	TRIF084	622,781	97,082	2,028	Ph-Cal-Qz	12	0.34	0.05	488	6
	TRIF085	622,163	97,333	2,268	Gt-Ep-Chl-Ph-Pl-Qz	10	0.33	0.04	494	6
	TRIF086	621,600	97,846	2,375	Ph-Pl-Cal-Qz	10	0.37	0.02	476	3
	TRIF087	621,650	97,283	2,478	Ep-Ph-Pl-Qz	14	0.50	0.03	421	4
	TRIF088	622,138	96,831	2,554	Ep-Ph-Pl-Cal-Qz	–	–	–	–	–
	TRIF0811	622,144	97,371	2,251	Ep-Ph-Cal-Qz	10	0.31	0.05	503	8
	TRIF0812	622,032	97,573	2,293	Ep-Ph-Cal-Qz	14	0.35	0.05	485	5
	Z081	624,087	97,455	1,886	Ep-Ph-Cal-Qz	10	0.36	0.05	480	8
	JES46	627,779	96,799	3,066	Grt-Pl-Chl-Ph-Cal-Qz	12	0.27	0.06	523	7
	JES59	628,577	96,163	2,719	Grt-Cld-Ph-Chl-Cal-Qtz	–	–	–	–	–
	JES142	628,356	96,945	2,956	Ep-Pl-Chl-Ph-Cal-Qz	16	0.31	0.07	504	8
	JES149	628,295	97,117	2,944	Pl-Chl-Ph-Qz	11	0.32	0.07	498	8
	JES218	627,415	97,583	2,892	Pl-Chl-Ph-Qz	19	0.31	0.08	503	8
	JES150a	628,579	96,172	2,715	Grt-Cld-Pl-Chl-Ph-Cal-Qz	12	0.29	0.04	511	5
	JES152_1	629,344	97,073	3,221	Grt-Ph-Chl-Qz	15	0.28	0.08	516	9
	JES246	628,164	97,656	2,871	Grt-Cld-Ph-Chl-Qtz	–	–	–	–	–

Table 1 continued

Coord. (CH1903)						R2 ratio		Temperature (°C)		
Zone/Unit	Sample	X	Y	Elev. (m)	Mineral assemblage	Sp	Mean	SD	Mean	1 s
Lower unit	SZ081	620,628	93,185	2,600	Grt-Ep-Ph-Cal-Qz	12	0.25	0.05	528	6
	SZ083	620,326	93,193	2,680	Ep-Ph-Pl-Qz	10	0.33	0.06	495	8
	FU082	622,437	94,509	1,895	Grt-Cld-Ph-Ep/Czo-Pl-Cal-Qtz	–	–	–	–	–
	FU084	622,281	94,394	1,965	Grt-Ep-Chl-Ph-Cal-Qz	12	0.24	0.03	535	4
	FU085	622,208	94,344	1,998	Grt-Cld-Ph-Czo-Cal-Qtz	–	–	–	–	–
	TS081	622,319	91,200	2,852	Grt-Ep-Chl-Ph-Qz	10	0.29	0.05	510	7
	TS082	622,046	91,868	2,684	Grt-Gln-Ep-Tr-Ph-Qz	12	0.24	0.06	536	8
	GOL081	626,848	92,474	3,128	Ph-Cal-Qz	10	0.27	0.05	521	7
	GOL087	625,198	92,638	2,797	Grt-Cld-Ph-Cal-Qz	10	0.25	0.06	531	9
	GOL088	625,067	92,780	2,770	Grt-Cld-Ph-Czo/Ep-Cal-Qtz	–	–	–	–	–
	GOL089	624,949	92,882	2,738	Grt-Ph-Cal-Qz	11	0.26	0.06	526	8
	GOL0812	624,653	93,581	2,612	Grt-Cld-Ph-Pl-Cal-Qz	12	0.22	0.05	543	7
	GOL0813	624,888	93,731	2,609	Grt-Ph-Chl-Ep/Czo-Pl-Cal-Qtz	–	–	–	–	–
	JES138	626,395	96,072	2,370	Grt-Pl-Chl-Ph	14	0.23	0.06	539	9
Lago di Cignana										
Upper unit	CIG0901	612885	80869	2279	Gt-Cld-Chl-Ph-Czo/Ep-Qz	12	0.25	0.04	532	6
	CIG0902	612868	80970	2358	Gt-Chl-Ph-Qz	15	0.34	0.07	498	5
	CIG0903	612865	80994	2385	Gt-Cld-Chl-Ph-Czo/Ep-Qz	15	0.31	0.04	504	5
	CIG0904	611516	80766	2160	Cld-Chl-Ph-Czo/Ep-Qz	10	0.30	0.05	506	8
	CIG0907	612379	82341	2504	Chl-Ph-Czo/Ep-Qz	9	0.37	0.03	475	5
	CIG0908	612340	82232	2465	Ph-Chl-Pl-Qz	15	0.39	0.04	466	5
	CIG0909	612312	82173	2465	Czo-Ph-Chl-Pl	–	–	–	–	–
	CIG0912	612576	81398	2590	Ph-Chl-Pl-Qz	13	0.30	0.06	508	8
	CIG0913	612310	81753	2523	Ph-Chl-Pl-Qz	12	0.39	0.03	469	4
	CIG0914	612283	81884	2493	Czo-Ph-Chl-Pl-Qz	14	0.42	0.03	455	4
	CIG0915	612314	82025	2468	Czo-Ph-Chl-Pl-Qz	–	–	–	–	–
	CIG0916	612295	82120	2449	Ph-Chl-Pl-Qz	10	0.37	0.04	474	6
	CIG0917	611195	81822	2170	Czo-Ph-Chl-Pl-Cal-Qz	13	0.38	0.03	474	4
	CIG1001	611516	80766	2160	Cld-Ep/Czo-Chl-Ph-Cal-Qz	15	0.29	0.06	513	7
Lower unit	CIG1002	611516	80766	2160	Czo-Ph-Chl-Cal-Qz	14	0.27	0.05	522	6
	CIG1003	613102	80146	1790	Czo-Ph-Chl-Cal-Qz	15	0.22	0.05	541	6

The absolute uncertainty on RSCM temperature is ±50 °C. Mineral abbreviations after Whitney and Evans (2010)

5 New metamorphic data in the Piemont-Ligurian metasediments

In addition to the estimation of peak T by the RSCM method, we studied systematically the mineral assemblage of each sample analysed. We also included some additional samples in order to complete the regional distribution of mineral assemblages (Figs. 2, 3 and 6). The mineral assemblages for all these samples are given in Table 1. Electron microprobe analysis of the most significant minerals assemblages were also performed using JEOL JXA8200 (University of Bern) and JEOL JXA8600 (University of Basel) using standard conditions (15 kV, 10 nA). Representative analyses of mineral assemblages in metasediments are given in Table 2.

5.1 Spatial distribution of mineral assemblages

Occurrence of mineral assemblages representative of HP conditions is scarce in metasediments of both units. Most of these metasediments are composed of quartz, calcite, phengite, with variable amounts of epidote, clinozoisite and plagioclase (Figs. 2, 3, 6; Table 1). In the area located north of the Dent Blanche nappe, relic garnet was only found in one sample from a metabasite south of Zinal (Fig. 2). In the Zermatt and Lago di Cignana areas, some samples depict a well preserved mineralogy, with garnet-chloritoid-phengite assemblage (Figs. 3, 6, 8a and b). This mineral assemblage is only observed locally, below the Ho¨rnlihu¨tte along the Matterhorn-Schwarwee profile (Fig. 3), in the Oberrothorn area (Fig. 3), and in the lower

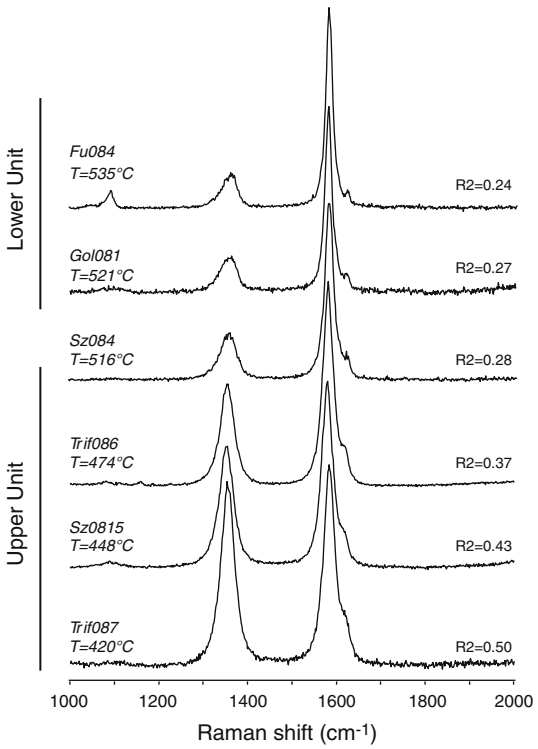

Fig. 4 Representative Raman spectra obtained from samples collected in the upper and lower units of the Piemont-Ligurian domain. The R2 ratio value and corresponding temperature are given for each spectra. Location of the samples in Fig. 3 and Table 1

part of the Lago di Cignana profile (Fig. 6a-b). This mineral assemblage has been found both in the LU associated to eclogites and in the UU without eclogites (Figs. 3, 8a–c). The most common mineral assemblage in the UU is Ph-Chl-Cal-Qz ± Ep/Czo ± Plg (Figs. 2, 3, 6 and Table 1) typical of greenschist facies metamorphic conditions. At the regional scale, field occurrences of mineral assemblages evidencing HP metamorphism are decreasing toward the west, where the overprinting seems to be predominant (Figs. 2, 3). They can be only found as relic garnet or sometimes chloritoid inclusions in albite porphyroblasts (Fig. 8e).

5.2 Mineral compositions and textural relationships

The main foliation in metapelites is defined by the alignment of phengite within a calcite-quartz matrix. Plagioclase frequently occurs as sheared porphyroblasts within the main foliation together with epidote and/or clinozoisite (Fig. 8f). Chloritoid is found as inclusion in big garnet pseudomorphs (Fig. 8a) together with phengite and chlorite, or within the main phengite foliation (Fig. 8b). The chloritoid compositions are homogeneous with an X_{Mg} in the range of 0.14–0.17 (Table 2). Different types of garnet have been observed in the UU samples, with regional consistency from Zermatt to Lago di Cignana (Figs. 3, 6; Table 2). Garnet porphyroblasts (type I) occur within the main foliation and show compositional zoning (Fig. 8b). The spessartine component is higher and the almandine component lower in the core of these garnets, compared to their rim (Table 2). Such kind of variation has been interpreted as a growth of garnet under increasing temperature conditions (Spear and Markussen 1997; Enami 1998; Tinkham and Ghent 2005). Smaller garnets (type II) occur within the main foliation (Fig. 8b) and their composition is similar to the rim of type I garnets (Table 2). Phengite associated with chloritoid and garnet within garnet pseudomorphs (Fig. 8a) or in garnet crystallization tail (Fig. 8b) show Si content in the range 3.38–3.46 (Table 2). Chlorite is found associated with chloritoid and phengite garnet within garnet pseudomorphs (Fig. 8a), in garnet crystallization tails (Fig. 8b, d–f), or within the main foliation, and show compositions with X_{Mg} in the range 0.43–0.46 (Table 2). Garnets partially (Fig. 8d) or almost totally (Fig. 8e) replaced by chlorite and plagioclase, are observed in some sample showing distinctive stages of retrograde evolution. Figure 8f depicts the most common assemblage and textural relationships observed in the UU samples.

6 Discussion

6.1 Metamorphic evolution of Piemont-Ligurian metasediments

The new petrological data on metasediments and their metamorphic record allow us to discuss the metamorphic evolution of the Piemont-Ligurian domain. The garnet-chloritoid-phengite assemblages, and their mineral compositions, are characteristic of blueschist facies metamorphic conditions in metasediments (Bousquet et al. 2008; Bucher and Grapes 2011). Peak P–T conditions of ∼12–15 kbar and ∼450 °C were estimated for the UU in the area of Zermatt in metabasites and metapelites (Cartwright and Barnicoat 2002; Bousquet et al. 2008). We therefore use these maximum P–T conditions (Fig. 9). Metasediments of the Piemont-Ligurian domain towards the south, north of the Gran Paradiso massif (Fig. 1), show similar petrological and metamorphic features. Indeed, the mineral assemblages, the mineral compositions and the textural relationships are very similar to our study (Bousquet 2008). Two distinct metamorphic stages, a LT-HP followed by heating during decompression have been identified. The P–T conditions are estimated for the first stage at 14 kbar and 450 ° C for primary garnet core associated with chloritoid and primary phengite and for the second one at 7–8 kbar and 530 ° C for secondary garnet

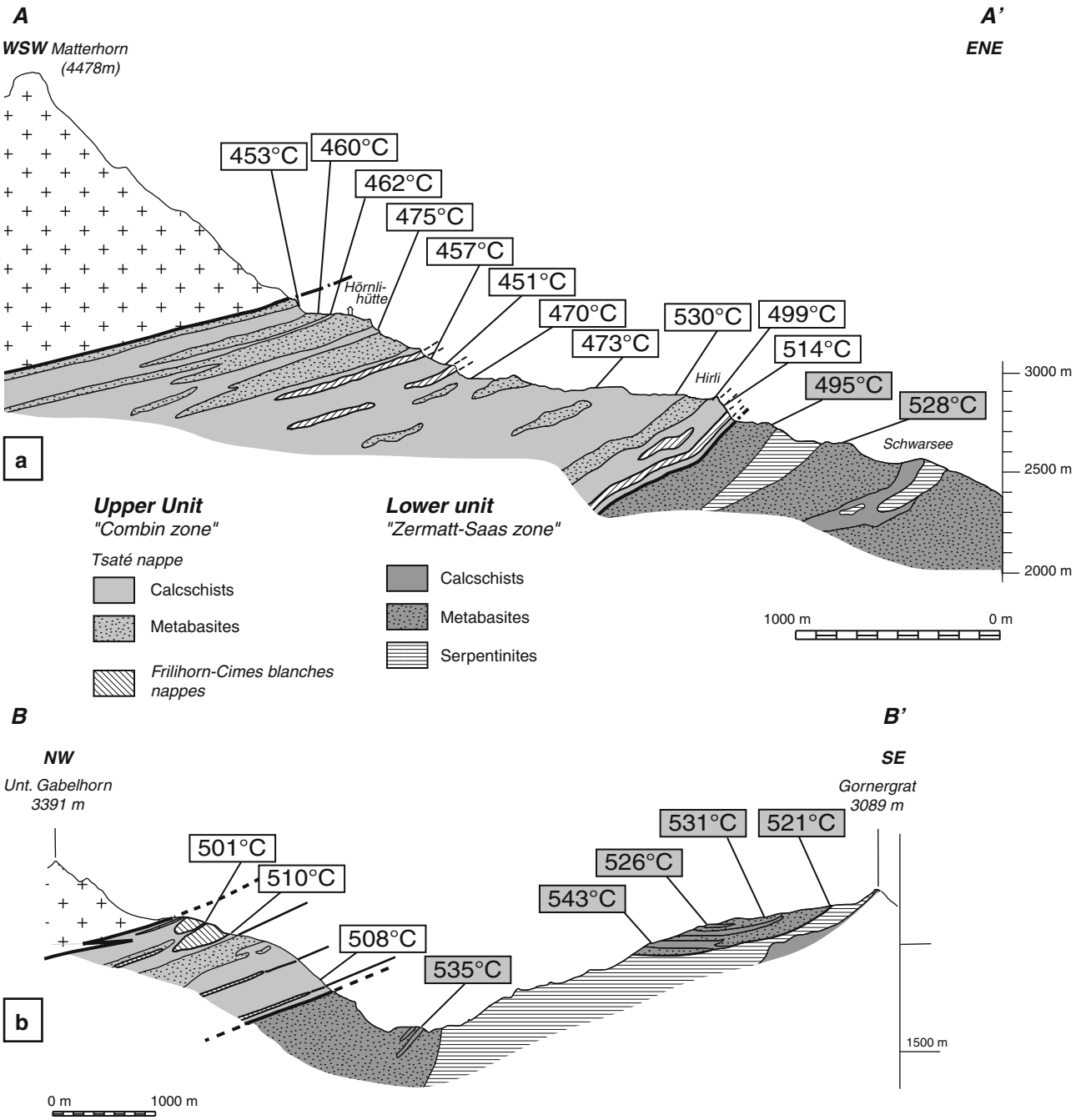

Fig. 5 **a** Simplified geological cross-section between Schwarzee and Matterhorn showing the distribution of RSCM temperatures upper and lower units of the Piemont-Ligurian domain (modified after Bucher et al. 2004). **b** Simplified geological cross-section between Unter Gabelhorn and Gornergrat showing the distribution of RSCM temperatures in the upper and lower units of the Piemont-Ligurian domain (modified after Bearth 1953). The cross-sections are located in Fig. 3. The absolute uncertainty on RSCM temperatures is ±50 °C

associated with clinozoisite, chlorite and secondary phengite. On the basis of these data and our own investigations, we propose a P–T evolution for metasediments similar to the Zermatt area (Fig. 9). This will serve as a basis to discuss and interpret the observed thermal structure.

6.2 RSCM temperatures and metamorphic evolution

In the lower levels of the UU, estimated temperatures are very consistent in the range of 500–530 °C. On the basis of the textural relationships and garnet compositional zoning, we relate these RSCM temperatures to the growth of

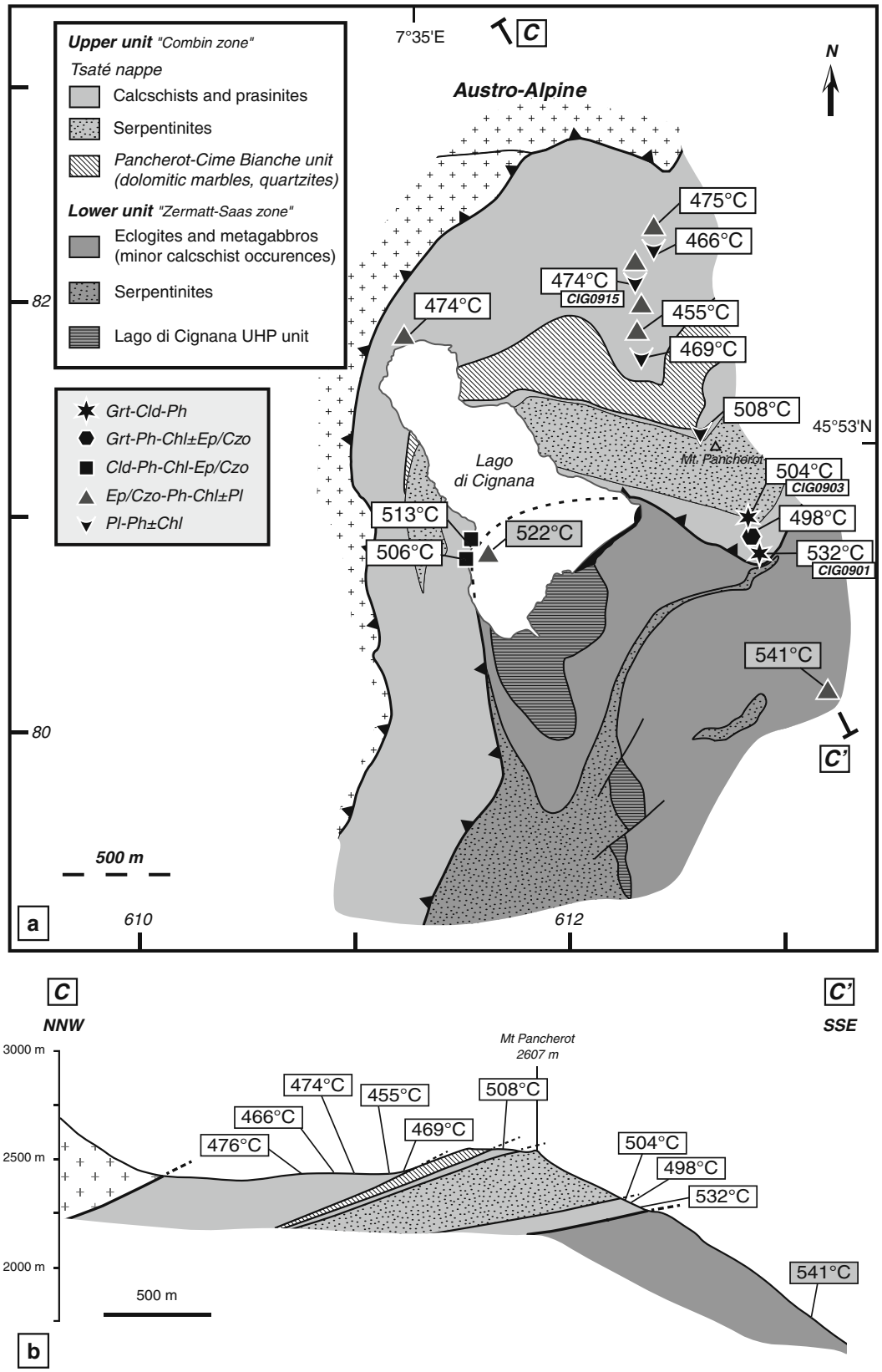

Fig. 6 Tectonic map of the Lago di Cignana area (modified after Compagnoni and Rolfo 2003) showing RSCM temperatures and metamorphic assemblages in the upper and lower units of the Piemont-Ligurian domain. The absolute uncertainty on RSCM temperatures is ±50 °C

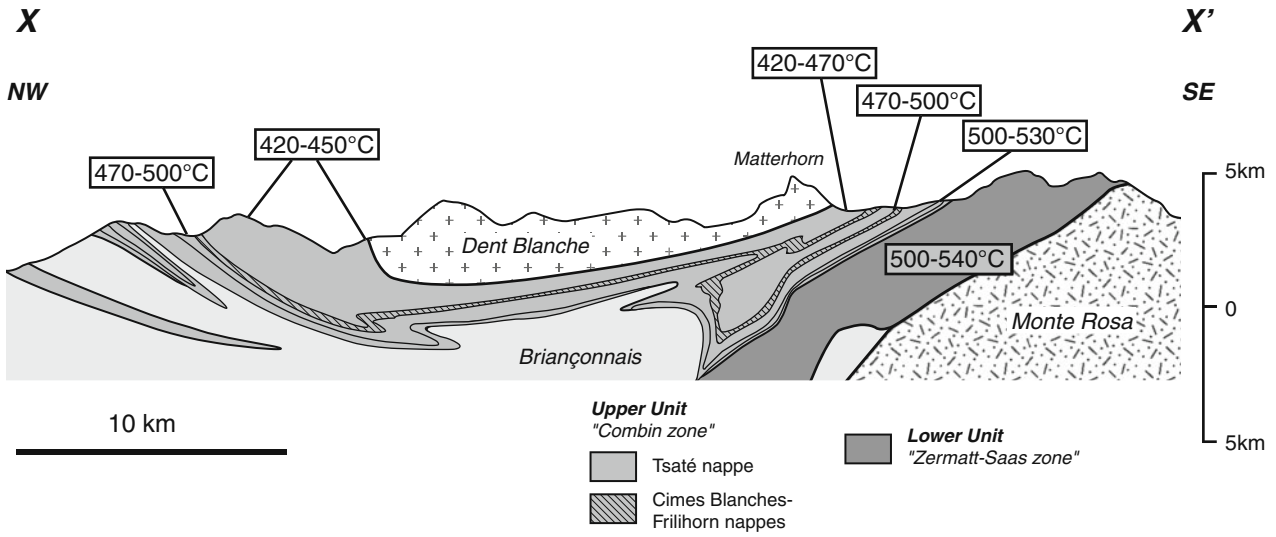

Fig. 7 Simplified geological cross section across the Penninic units of the northern Western Alps (modified after Escher et al. 1993) showing the range of estimated RSCM temperatures estimated in the upper and lower units of the Piemont-Ligurian domain. The cross section is located in Fig. 2

Table 2 Representative electron microprobe analysis of mineral assemblages in the upper unit

Sample	CIG0901				CIG0903						Jes59			
Mineral	Grt	Cld	Ph	Chl	Grt I (core)	Grt I (rim)	Grt II	Cld	Ph	Chl	Grt (core)	Grt (rim)	Cld	Ph
SiO_2	37.99	24.82	50.88	24.58	37.55	37.95	37.11	24.75	50.20	24.84	37.08	37.31	24.55	51.24
TiO_2	0.00	0.00	0.18	0.06	0.13	0.06	0.05	0.00	0.20	0.03	0.16	0.00	0.00	0.20
Al_2O_3	21.01	42.14	28.28	23.34	20.89	21.15	21.29	41.77	27.86	23.63	20.40	20.36	38.42	25.89
FeO	29.40	24.90	2.47	28.55	13.53	27.94	27.18	22.89	2.58	26.65	24.17	30.52	25.34	2.62
MnO	0.81	0.38	0.00	0.07	19.30	3.72	6.21	1.39	0.03	0.80	12.02	5.78	0.76	0.01
MgO	1.20	2.29	2.92	12.32	0.42	1.07	1.26	2.74	2.86	13.06	0.87	1.27	2.68	3.25
CaO	9.94	0.00	0.00	0.02	8.02	8.93	6.81	0.00	0.01	0.01	6.08	5.64	0.02	0.00
Na_2O	0.04	0.00	0.36	0.01	0.03	0.04	0.01	0.01	0.35	0.02	0.07	0.02	0.02	0.26
K_2O	0.00	0.00	10.39	0.07	0.00	0.00	0.00	0.00	9.92	0.05	0.00	0.00	0.00	10.95
Total	100.39	94.53	95.48	89.02	99.87	100.86	99.92	93.55	94.01	89.09	100.85	100.90	91.79	94.42
Structural formula														
Si	3.02	2.00	3.38	2.59	3.03	3.02	2.99	2.01	3.39	2.60	2.99	3.01	2.06	3.46
Ti	0.00	0.00	0.01	0.00	0.01	0.00	0.00	0.00	0.01	0.00	0.01	0.00	0.00	0.01
Al	1.97	4.01	2.22	2.90	1.99	1.98	2.02	4.00	2.21	2.91	1.94	1.93	3.80	2.06
Fe^{2+}	1.96	1.68	0.14	2.52	0.91	1.86	1.83	1.55	0.15	2.33	1.63	2.06	1.58	0.15
Mn	0.05	0.03	0.00	0.01	1.32	0.25	0.42	0.10	0.00	0.07	0.82	0.39	0.05	0.00
Mg	0.14	0.28	0.29	1.94	0.05	0.13	0.15	0.33	0.29	2.03	0.10	0.15	0.34	0.33
Ca	0.85	0.00	0.00	0.00	0.69	0.76	0.59	0.00	0.00	0.00	0.53	0.49	0.00	0.00
Na	0.01	0.00	0.05	0.00	0.00	0.01	0.00	0.00	0.05	0.00	0.01	0.00	0.00	0.03
K	0.00	0.00	0.88	0.01	0.00	0.00	0.00	0.00	0.85	0.01	0.00	0.00	0.00	0.94
X_{Mg}		0.14		0.43				0.17		0.46			0.17	
X_{Prp}	0.05				0.02	0.04	0.05				0.03	0.05		
X_{Alm}	0.65				0.31	0.62	0.61				0.53	0.67		
X_{Grs}	0.28				0.23	0.25	0.20				0.17	0.16		
X_{Sps}	0.02				0.44	0.08	0.14				0.27	0.13		

Samples are located in Figs. 3 and 6

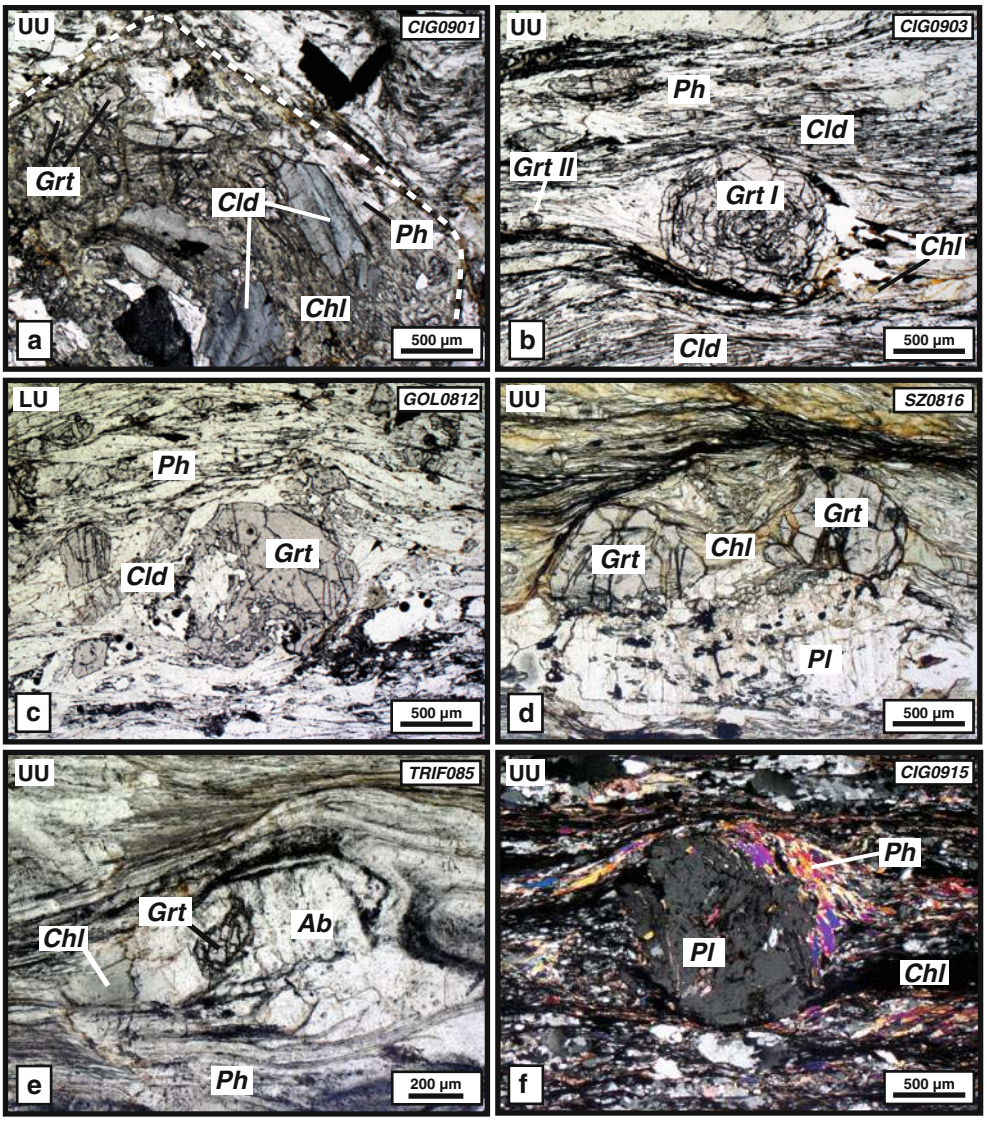

Fig. 8 Photomicrographs of the metamorphic assemblages observed in the metasediments of the upper and lower units of the Piemont-Ligurian domain. Samples are located in Figs. 3 and 6 and Table 1. **a** Garnet relic with chloritoid and chlorite inclusion in the CIG0901 sample at Lago di Cignana (plane polarized light). **b** Garnet-chloritoid-phengite assemblage in the CIG0903 sample at Lago di Cignana (plane polarized light). **c** Garnet chloritoid-phengite assemblage in the GOL0812 sample at Gornergrat (plane polarized light). **d** Garnet partially replaced by chlorite and albite in the SZ0816 sample near Ho¨rnlihu¨tte (plane polarized light). **e** Relic garnet within albite porphyroblasts in the TRIF0805 sample near Trift (plane polarized light). **f** Sheared albite porphyroblast in the chlorite-phengite foliation in the CIG0915 sample at Lago di Cignana (*crossed polars*). Mineral abbreviations after Whitney and Evans (2010)

secondary garnet within the main foliation. This interpretation is also in agreement with temperatures estimated by classical thermobarometry by Bousquet (2008). We therefore propose that the estimated RSCM temperatures in the range of 500–530 ° C, observed at the base of the UU, likely correspond to heating during exhumation of metasediments (Fig. 9).

In the upper levels of the UU, at first sight, mineral assemblages are documenting greenschist facies conditions, and RSCM temperatures ranging between 420 and 500 °C are indicating similar T-conditions (Figs. 3, 5a, b). Along the Zermatt-Trift profile (Fig. 5b), the Tsate´ and Frilihorn nappes are intensely deformed and folded (Bearth 1967; Mazurek 1986; Sartori 1987) and the temperature is very homogenous along this profile (480–500 ° C). The temperature range of 480–500 ° C also corresponds to temperature estimated in sheared calcschists in the Ta¨s-chalp region for a pressure of ∼5 kbar (Cartwright and Barnicoat 2002). Based on HP-relics in plagioclase, we therefore interpret RSCM temperatures as documenting the reheating during decompression. The more pervasive greenschist retrogression in this area (Figs. 3, 8e) was also favoured by more intensive deformation during exhumation.

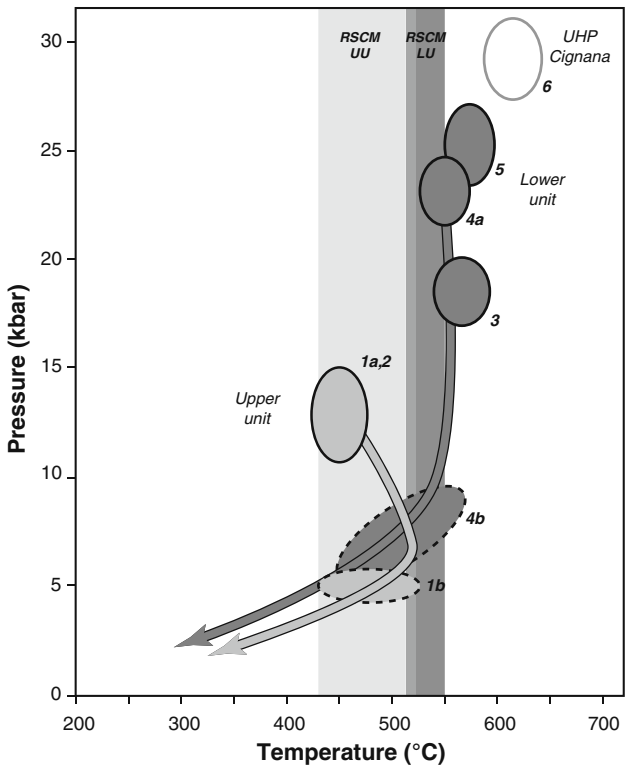

Fig. 9 Synthetic P–T grid for the Piemont-Ligurian units with proposed P–T evolution for the different tectono-metamorphic units. P–T conditions after: *1a,b* Cartwright and Barnicoat (2002); *2* Bousquet et al. (2008); *3* Oberha¨nsli (1980), Barnicoat and Fry (1986); *4a,b* Angiboust et al. (2009); *5* Bucher et al. (2005); *6* Reinecke (1991), Groppo et al. (2009)

6.3 Thermal structure and exhumation history of the Piemont-Ligurian units

The RSCM temperatures obtained for the LU are slightly lower but in good agreement with previous P–T estimates obtained with geothermobarometry (Bucher et al. 2005). According to Angiboust et al. (2009) the LU underwent nearly isothermal decompression from 24 to ~6–8 kbar at a temperature of ~550 ° C. The RSCM temperatures therefore correspond to near peak P–T conditions. According to the P–T paths (Fig. 9), the different units were juxtaposed at a shallow crustal level within a sub-duction channel. This P–T evolution suggests that the UU and the LU were put together at a depth of ~15–20 km and a temperature of ~500 °C. This juxtaposition occurred along several shear zones (limits of the different units), that were active during the Middle Eocene (~40–35 Ma; Reddy et al. 1999; Cartwright and Barnicoat 2002). The difference in thermal overprint during exhumation may also evidence a change of the thermal gradient during nappe stacking in this period. Our study, associated with the diamond discovery in the Lago di Cignana UHP unit (Frezzotti et al. 2011), clearly shows that the different units of the Piemont-Ligurian domain in the northern Western Alps cannot longer be viewed as a juxtaposition of only two distinct ''zones''. Finally, considering similar observation in the Graian Alps (Bousquet 2008) and in the Cottian Alps (Agard et al. 2001), we propose that the entire Piemont-Ligurian domain of the Western Alps is a stack of several tectonics slices with distinctive prograde and retrograde metamorphic evolution.

7 Conclusion

The results of this study based on a combined petrological and RCSM study provide new constraints on the metamorphic evolution of the Piemont-Ligurian domain in the northern Western Alps. The RSCM temperature distribution is coherent at a regional scale in the Piemont-Ligurian domain. The metasediments of the upper unit, or "Combin zone", show variable peak temperatures in the range of 420–530 °C, with an increase in temperature from upper to lower structural levels. This temperature is related to greenschist metamorphic conditions and deformation during exhumation. Metamorphic data highlight an increase in temperature during retrograde evolution from blueschist to greenschist facies metamorphic conditions. The temperatures observed in the lower unit, or "Zermatt-Saas zone", are in the range of 500–540 °C, showing almost continuous temperature record in the upper and lower units of the Piemont-Ligurian domain. We interpret the observed thermal structure as the result of juxtaposition of the upper and lower units along shear zones at a temperature of ~500 °C during the Middle Eocene. According to the proposed P–T paths for the different units, this juxtaposition occurred at shallow crustal levels within a subduction channel. At a larger scale, we propose that the Piemont-Ligurian Domain is not only composed of two units, separated by a major contact, but represents a stack of several tectonic slices with their own metamorphic history accreted together during the subduction.

Acknowledgments The French-Swiss program "Germaine de Stael" is thanked for financial support during field and laboratory work. We warmly thank O. Beyssac (IMPMC, Paris), C. Chopin (ENS, Paris) and R. Oberhänsli (Uni. Potsdam) for accessing Raman spectroscopy facilities. We also thank A. Villard for the quality and number of thin sections. Kurt Bucher and Michael Wiederkehr are acknowledged for their constructive comments that greatly improved the manuscript.

References

Agard, P., Jolivet, L., & Goffé, B. (2001). Tectonometamorphic evolution of the Schistes Lustres complex: Implications for the

exhumation of HP and UHP rocks in the western Alps. *Bulletin de la Société Géologique de France, 172*(5), 617–636.

Angiboust, S., Agard, P., Jolivet, L., & Beyssac, O. (2009). The Zermatt-Saas ophiolite: The largest (60-km wide) and deepest (c. 70–80 km) continuous slice of oceanic lithosphere detached from a subduction zone? *Terra Nova, 21*(3), 171–180.

Aoya, M., Kouketsu, Y., Endo, S., Shimizu, H., Mizukami, T., Nakamura, D., et al. (2010). Extending the applicability of the Raman carbonaceous-material geothermometer using data from contact metamorphic rocks. *Journal of Metamorphic Geology, 28*(9), 895–914.

Argand, E. (1909). L'exploraiton géologique des Alpes Pennines centrales. *Bulletin de la Société Vaudoise des Sciences naturelles, 45*, 217–276.

Ayrton, S., Bugnon, C., Haarpaintner, T., Weidmann, M., & Frank, E. (1982). Géologie du front de la nappe de la Dent Blanche dans la région des Monts Dolins, Valais. *Eclogae Geologicae Helvetiae, 75*(2), 269–286.

Ballèvre, M., & Merle, O. (1993). The Combin Fault—compressional reactivation of a Late Cretaceous-Early Tertiary detachment fault in the Western Alps. *Schweizerische Mineralogische und Petrographische Mitteilungen, 73*(2), 205–227.

Barnicoat, A. C., & Fry, N. (1986). High-pressure metamorphism in the Zermatt-Saas zone of the Swiss Alps. *Journal of the Geological Society, 143*, 607–618.

Bearth, P. (1953). *Blatt 535 Zermatt - Geologischer Atlas der Schweiz 1:25 000*. Bern: Commission géologique Suisse.

Bearth, P. (1959). Über Eklogite, Glaukophanschiefer und metamorphe Pillowlaven. *Schweizerische Mineralogische und Petrographische Mitteilungen, 39*, 267–286.

Bearth, P. (1967). Die Ophiolite der zone von Zermatt-Saas Fee. *Beiträge zur geologischen Karte der Schweiz (NF)*, *132*, 130 pp.

Bearth, P. (1976). Zur Gliederung der Bündnerschiefer in der Region von Zermatt. *Eclogae Geologicae Helvetiae, 69*(1), 149–161.

Bearth, P., & Schwander, H. (1981). The post-Triassic sediments of the ophiolite zone Zermatt-Saas Fee and the associated manganese mineralizations. *Eclogae Geologicae Helvetiae, 74*(1), 189–205.

Beltrando, M., Lister, G., Hermann, J., Forster, M., & Compagnoni, R. (2008). Deformation mode switches in the Penninic units of the Urtier Valley (Western Alps): Evidence for a dynamic orogen. *Journal of Structural Geology, 30*(2), 194–219.

Beyssac, O., Goffé, B., Chopin, C., & Rouzaud, J. N. (2002). Raman spectra of carbonaceous material in metasediments: A new geothermometer. *Journal of Metamorphic Geology, 20*(9), 859–871.

Beyssac, O., Goffé, B., Petitet, J. P., Froigneux, E., Moreau, M., & Rouzaud, J. N. (2003). On the characterization of disordered and heterogeneous carbonaceous materials by Raman spectroscopy. *Spectrochimica Acta Part A-Molecular and Biomolecular Spectroscopy, 59*(10), 2267–2276.

Bousquet, R. (2008). Metamorphic heterogeneities within a single HP unit: Overprint effect or metamorphic mix? *Lithos, 103*(1–2), 46–69.

Bousquet, R., Engi, M., Gosso, G., Oberhänsli, R., Berger, A., Iole Spalla, M., et al. (2004). Explanatory notes to the map: Metamorphic structure of the Alps. Transition from the Western to the Central Alps. *Mitteilungen der Österreichischen Mineralogischen Gesellschaft, 149*, 145–156.

Bousquet, R., Oberhänsli, R., Goffé, B., Wiederkehr, M., Koller, F., Schmid, S. M., et al. (2008). Metamorphism of metasediments at the scale of an orogen: A key to the Tertiary geodynamic evolution of the Alps. In S. Siegesmund, B. Füngenschuh, & N. Froitzheim (Eds.), *Tectonic Aspects of the Alpine-Dinaride-Carpathian System, 298* (pp. 393–411). London: Geological Society of London, Special Publications.

Bousquet, R., Oberhänsli, R., Schmid, S. M., Berger, A., Wiederkehr, M., Robert, C., Möller, A., Rosenberg, C., Zeilinger, G., Molli, G. and Koller, F. (2012a). Metamorphic map of the Alps - 1/1.000.000. Paris: Commission for the Geological Map of the World.

Bousquet, R., Schmid, S. M., Zeilinger, G., Oberhänsli, R., Rosenberg, C., Molli, G., Robert, C., Wiederkehr, M. & Rossi, P. (2012b). Tectonic map of the Alps - 1:1.000.000. Paris: Commission for the Geological Map of the World.

Bucher, K., Dal Piaz, G. V., Oberhänsli, R., Gouffon, Y., Martinotti, G., & Polino, R. (2003). *Blatt 1347 Matterhorn - Geologischer Atlas der Schweiz 1:25 000, Karte 107*. Bern: Bundesamt fur Wasser und Geologie.

Bucher, K., Dal Piaz, G. V., Oberhänsli, R., Gouffon, Y., Martinotti, G., & Polino, R. (2004). *Blatt 1347 Matterhorn - Geologischer Atlas der Schweiz 1:25 000, Erläuterungen 107*. Bern: Bundesamt fur Wasser und Geologie.

Bucher, K., Fazis, Y., De Capitani, C., & Grapes, R. (2005). Blueschists, eclogites, and decompression assemblages of the Zermatt-Saas ophiolite: High-pressure metamorphism of subducted Tethys lithosphere. *American Mineralogist, 90*(5–6), 821–835.

Bucher, K. & Grapes, R. (2011). *Petrogenesis of metamorphic rocks* (428 pp.). Berlin: Springer.

Cartwright, I., & Barnicoat, A. C. (2002). Petrology, geochronology, and tectonics of shear zones in the Zermatt-Saas and Combin zones of the Western Alps. *Journal of Metamorphic Geology, 20*(2), 263–281.

Compagnoni, R. & Rolfo, F. (2003). UHPM units in the Western Alps. In D. A. Carswell and R. Compagnoni (Eds.), *Ultra High Pressure Metamorphism* (pp. 13–45). European Mineralogical Union Notes in Mineralogy 5.

Dal Piaz, G. V. (1965). La formation mesozoica dei calcescisti con pietre verdi fra la Valsesia e la Valtournanche ed i suoi rapporti strutturali con il ricoprimento Monte Rosa et con la zona Sesia-Lanzo. *Bolletion de la Societa Geologica Italiana, 84*, 67–104.

Dal Piaz, G. V. (1988). Revised setting of the Piedmont zone in the northern Aosta Valley, Western Alps. *Ofioliti, 13*(2/3), 157–162.

Dal Piaz, G. V., & Ernst, W. G. (1978). Areal geology and petrology of eclogites and associated metabasites of Piemonte Ophiolite nappe, breuil-st Jacques area, Italian Western Alps. *Tectonophysics, 51*(1–2), 99–126.

Enami, M. (1998). Pressure-temperature path of Sanbagawa prograde metamorphism deduced from grossular zoning of garnet. *Journal of Metamorphic Geology, 16*(1), 97–106.

Ernst, W. G., & Dal Piaz, G. V. (1978). Mineral parageneses of eclogitic rocks and related mafic schists of Piemonte ophiolite nappe, breuil-St-Jacques area, Italian Western Alps. *American Mineralogist, 63*(7–8), 621–640.

Escher, A., Masson, H., & Steck, A. (1993). Nappe Geometry in the Western Swiss Alps. *Journal of Structural Geology, 15*(3–5), 501–509.

Forster, M., Lister, G., Compagnoni, R., Giles, D., Hills, Q., Betts, P., et al. (2004). Mapping of oceanic crust with "hp" to "uhp" metamorphism: The Lago di Cignana unit (Western Alps). In G. Pasquare, C. Venturini, & G. Groppelli (Eds.), *Mapping geology in Italy* (pp. 279–286). Roma: Servizio Geologico d'Italia.

Frezzotti, M. L., Selverstone, J., Sharp, Z. D., & Compagnoni, R. (2011). Carbonate dissolution during subduction revealed by diamond-bearing rocks from the Alps. *Nature Geoscience, 4*(10), 703–706.

Froitzheim, N., Pleuger, J., & Nagel, T. J. (2006). Extraction faults. *Journal of Structural Geology, 28*(8), 1388–1395.

Groppo, C., Beltrando, M., & Compagnoni, R. (2009). The P-T path of the ultra-high pressure Lago Di Cignana and adjoining high-pressure meta-ophiolitic units: Insights into the evolution of the

subducting Tethyan slab. *Journal of Metamorphic Geology, 27*(3), 207–231.

Lahfid, A., Beyssac, O., Deville, E., Negro, F., Chopin, C., & Goffe, B. (2010). Evolution of the Raman spectrum of carbonaceous material in low-grade metasediments of the Glarus Alps (Switzerland). *Terra Nova, 22*(5), 354–360.

Marthaler, M. (1984). Géologie des unités penniques entre le Val d'Anniviers et le Val de Tourtemagne (Valais, Suisse). *Eclogae Geologicae Helvetiae, 77*(2), 395–448.

Marthaler, M., & Stampfli, G. (1989). Les Schistes lustrés à ophiolites de la nappe du Tsaté: Un ancien prisme d'accrétion issu de la marge active apulienne? *Schweizerische Mineralogische und Petrographische Mitteilungen, 69*(2), 211–216.

Mazurek, M. (1986). Structural Evolution and Metamorphism of the Dent Blanche Nappe and the Combin Zone West of Zermatt (Switzerland). *Eclogae Geologicae Helvetiae, 79*(1), 41–56.

Negro, F., Beyssac, O., Goffé, B., Saddiqi, O., & Bouybaouène, M. L. (2006). Thermal structure of the Alboran Domain in the Rif (northern Morocco) and the Western Betics (southern Spain). Constraints from Raman spectroscopy of carbonaceous material. *Journal of Metamorphic Geology, 24*(4), 309–327.

Oberhänsli, R. (1980). PT Bestimmungen anhand von Mineralanalysen in Eklogiten und Glaukophaniten der Ophiolite von Zermatt. *Schweizerische Mineralogische und Petrographische Mitteilungen, 60*, 215–235.

Pfeifer, H.-R., Colombi, A., Ganguin, J., Hunziker, J., Oberhänsli, R., & Santini, L. (1991). Relics of high pressure metamorphism in different lithologies of the Central Alps, an updated inventory. *Schweizerische Mineralogische und Petrographische Mitteilungen, 71*, 441–451.

Pleuger, J., Roller, S., Walter, J. M., Jansen, E., & Froitzheim, N. (2007). Structural evolution of the contact between two Penninic nappes (Zermatt-Saas zone and Combin zone, Western Alps) and implications for the exhumation mechanism and palaeogeography. *International Journal of Earth Sciences, 96*(2), 229–252.

Rahl, J. M., Anderson, K. M., Brandon, M. T., & Fassoulas, C. (2005). Raman spectroscopic carbonaceous material thermometry of low-grade metamorphic rocks: Calibration and application to tectonic exhumation in Crete, Greece. *Earth and Planetary Science Letters, 240*(2), 339–354.

Reddy, S. M., Wheeler, J., Butler, R. W. H., Cliff, R. A., Freeman, S., Inger, S., et al. (2003). Kinematic reworking and exhumation within the convergent Alpine Orogen. *Tectonophysics, 365*(1–4), 77–102.

Reddy, S. M., Wheeler, J., & Cliff, R. A. (1999). The geometry and timing of orogenic extension: An example from the Western Italian Alps. *Journal of Metamorphic Geology, 17*(5), 573–589.

Reinecke, T. (1991). Very-high-pressure metamorphism and uplift of coesite-bearing metasediments from the Zermatt-Saas zone, Western Alps. *European Journal of Mineralogy, 3*(1), 7–17.

Reinecke, T. (1998). Prograde high- to ultrahigh-pressure metamorphism and exhumation of oceanic sediments at Lago di Cignana, Zermatt-Saas Zone, western Alps. *Lithos, 42*(3–4), 147–189.

Ring, U. (1995). Horizontal contraction or horizontal extension? Heterogeneous Late Eocene and Early Oligocene general shearing during blueschist and greenschist facies metamorphism at the Pennine-Austroalpine boundary zone in the Western Alps. *Geologische Rundschau, 84*(4), 843–859.

Rubatto, D., Gebauer, D., & Fanning, M. (1998). Jurassic formation and Eocene subduction of the Zermatt-Saas-Fee ophiolites: Implications for the geodynamic evolution of the Central and Western Alps. *Contributions to Mineralogy and Petrology, 132*(3), 269–287.

Sartori, M. (1987). Structure of the Combin Zone between the Diablons and Zermatt (Valais). *Eclogae Geologicae Helvetiae, 80*(3), 789–814.

Sartori, M., & Marthaler, M. (1994). Exemples de relations socle-couverture dans les nappes penniques du Val d'Hérens : Compte-rendu de l'excursion de la Société Géologique Suisse et de la Société Suisse de Minéralogie et Pétrographie (25 et 26 septembre 1993). *Schweizerische Mineralogische und Petrographische Mitteilungen, 74*(3), 503–509.

Spear, F. S., & Markussen, J. C. (1997). Mineral zoning, P-T-X-M phase relations, and metamorphic evolution of some Adirondack granulites, New York. *Journal of Petrology, 38*(6), 757–783.

Sperlich, R. (1988). The transition from crossite to actinolite in the metabasites of the Combin unit in Vallée St Barthélemy (Aosta, Italy). *Schweizerische Mineralogische und Petrographische Mitteilungen, 68*, 215–224.

Steck, A., Bigioggero, B., Dal Piaz, G. V., Escher, A., Martinotti, G., & Masson, H. (1999). Carte tectonique des Alpes de Suisse occidentale, 1:100 000. Carte géologique spéciale N°123. Berne: Service hydrogéologique et géologique national.

Tinkham, D. K., & Ghent, E. D. (2005). Estimating P-T conditions of garnet growth with isochemical phase-diagram sections and the problem of effective bulk-composition. *Canadian Mineralogist, 43*, 35–50.

Vannay, J.-C., & Alleman, R. (1990). La zone piémontaise dans le Haut-Valtournanche (Val d'Aoste, Italie). *Eclogae Geologicae Helvetiae, 83*(1), 21–39.

Whitney, D. L., & Evans, B. W. (2010). Abbreviations for names of rock-forming minerals. *American Mineralogist, 95*(1), 185–187.

Wiederkehr, M., Bousquet, R., Ziemann, M. A., Berger, A., & Schmid, S. M. (2011). 3-D assessment of peak-metamorphic conditions by Raman spectroscopy of carbonaceous material: An example from the margin of the Lepontine dome (Swiss Central Alps). *International Journal of Earth Sciences, 100*(5), 1029–1063.

Wopenka, B., & Pasteris, J. D. (1993). Structural characterization of kerogens to granulite facies graphite: Applicability of Raman microprobe spectroscopy. *American Mineralogist, 78*, 533–577.